Atmospheric correction of SeaWiFS ocean color imagery in the presence of absorbing aerosols off the Indian coast using a neuro-variational method

Julien Brajard, Cyril Moulin, Sylvie Thiria

Atmospheric correction of SeaWiFS ocean color imagery in the presence of absorbing aerosols off the Indian coast using a neuro-variational method

J. Brajard,[1] C. Moulin,[2] and S. Thiria[1]

Received 28 June 2008; revised 10 September 2008; accepted 15 September 2008; published 21 October 2008.

[1] This paper presents a comparison of the atmospheric correction accuracy between the standard sea-viewing wide field-of-view sensor (SeaWiFS) algorithm and the NeuroVaria algorithm for the ocean off the Indian coast in March 1999. NeuroVaria is a general method developed to retrieve aerosol optical properties and water-leaving reflectances for all types of aerosols, including absorbing ones. It has been applied to SeaWiFS images of March 1999, during an episode of transport of absorbing aerosols coming from pollutant sources in India. Water-leaving reflectances and aerosol optical thickness estimated by the two methods were extracted along a transect across the aerosol plume for three days. The comparison showed that NeuroVaria allows the retrieval of oceanic properties in the presence of absorbing aerosols with a better spatial and temporal stability than the standard SeaWiFS algorithm. NeuroVaria was then applied to the available SeaWiFS images over a two-week period. NeuroVaria algorithm retrieves ocean products for a larger number of pixels than the standard one and eliminates most of the discontinuities and artifacts associated with the standard algorithm in presence of absorbing aerosols. **Citation:** Brajard, J., C. Moulin, and S. Thiria (2008), Atmospheric correction of SeaWiFS ocean color imagery in the presence of absorbing aerosols off the Indian coast using a neuro-variational method, *Geophys. Res. Lett.*, *35*, L20604, doi:10.1029/2008GL035179.

1. Introduction

[2] Ocean color space borne sensors measure the reflectance of the ocean-atmosphere system. Inverting the reflectance allows the retrieval of information from the topmost water layer, for example the concentration of chlorophyll-*a* (chl-*a*) which is the predominant pigment in phytoplankton cells. The signal measured by the radiometer, corrected for Rayleigh scattering and gaseous absorption can be expressed as [*Gordon*, 1997]:

$$\rho_{cor}(\lambda) = \rho_A(\lambda) + t(\lambda) \times \rho_w(\lambda) \quad (1)$$

where $\rho_A(\lambda)$ is the atmospheric reflectance, $t(\lambda)$ is the atmospheric diffuse transmittance, $\rho_w(\lambda)$ is the water-leaving reflectance and λ specifies the wavelength of observation.

[3] Standard algorithms process ocean color images in three steps: The first step aims at determining the aerosol optical properties from ρ_{cor} in the red and near infrared bands where ρ_w is negligible. The second step, which is called the atmospheric correction, relies on the such determined aerosol optical properties to estimate ρ_A and t in the blue-green bands and to compute ρ_w in these bands using equation (1). The third and final step uses a bio-optical model to retrieve the chlorophyll-*a* concentration from ρ_w [*O'Reilly et al.*, 1998].

[4] Such standard algorithms [*Gordon*, 1997] give accurate estimates in most cases, but they fail in some specific situations, for example in presence of absorbing aerosols. This is because the effect of aerosol absorption on measured reflectances is stronger in the visible than in the near-infrared, as a result of a stronger coupling between molecular (Rayleigh) and aerosol scattering. Since the SeaWiFS standard algorithm [*Gordon and Wang*, 1994] relies only on near-infrared bands to derive the aerosol properties over the whole spectrum, it does not allow detecting aerosol absorption, so that only purely scattering aerosols are considered in most standard algorithms. This limitation induces an overestimation of ρ_A in the blue-green bands for absorbing aerosols and consequently an underestimation of ρ_w, which yields to an overestimation of the chl-*a* concentration [*Gordon*, 1997].

[5] Two methods, based on the same principle, were previously developed to address this issue: the Spectral Matching Algorithm or SMA [*Gordon et al.*, 1997], and the Spectral Optimization Algorithm or SOA [*Chomko and Gordon*, 2001]. SMA was validated for mineral dust off the African coast [*Moulin et al.*, 2001] and SOA for weakly absorbing pollutant aerosols off the East Coast of the USA [*Chomko and Gordon*, 1998] and for absorbing aerosols during the monsoon bloom of summer-fall 2000 in the Arabic Sea [*Banzon et al.*, 2004]. The main drawback of these two methods is that they are time-consuming and cannot be used for systematic processings of ocean color imagery. A new inversion method, called NeuroVaria, was developed to perform faster and more efficient atmospheric correction in the presence of both absorbing and non-absorbing aerosols [*Jamet et al.*, 2005; *Brajard et al.*, 2006a]. This algorithm combines neural network techniques based on multi-layer perceptrons (MLP) with a variational approach.

[6] The principle of NeuroVaria is fundamentally similar to that used in SMA and SOA [*Gordon et al.*, 1997; *Chomko and Gordon*, 2001], i.e., a global optimization of the whole spectrum of $\rho_{cor}(\lambda)$ is attempted by minimizing the difference between measured and simulated reflectances

[1] Laboratoire d'Océanographie et du Climat: Expérimentation et Approche Numérique, IPSL, Paris, France.
[2] Laboratoire des Sciences du Climat et de l'Environnement, CEA-Saclay, Gif-sur-Yvette, France.

0094-8276/08/2008GL035179

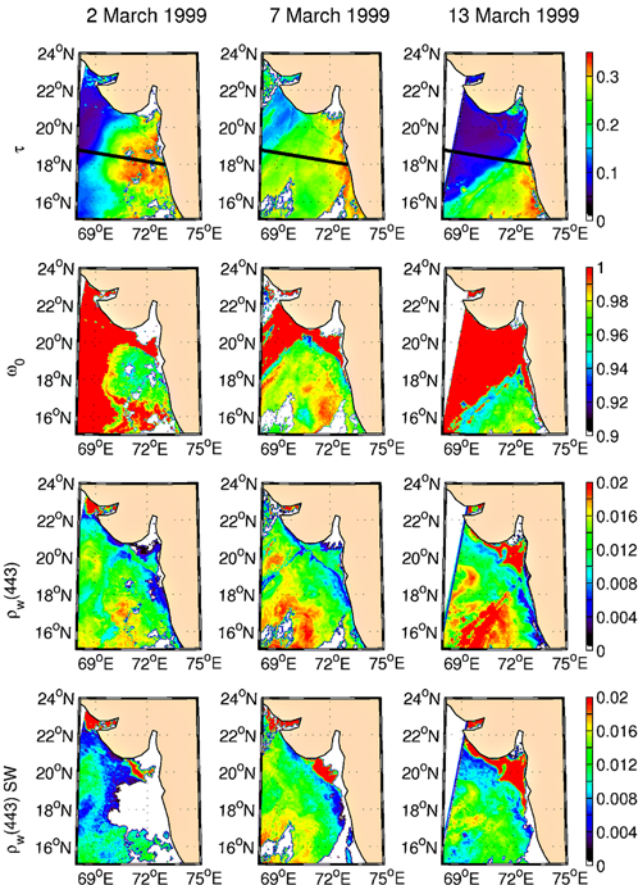

Figure 1. Daily maps (2, 7 and 13 March 1999) of aerosol optical thickness τ, single scattering albedo ω_0, the water-leaving reflectance $\rho_w(443)$ computed by NeuroVaria and $\rho_w(443)$ computed by the SeaDAS standard algorithm. White pixels are those where the algorithms failed. For 2 March 1999, absorbing aerosols were associated with a large optical thickness plume (18°N, 72.5°E). The solid black line in the first row represents the transect shown in Figure 3.

at all wavelengths. In addition, NeuroVaria relies on the same set of theoretical radiative transfer computations [*Chomko and Gordon*, 1998] than the two previous methods. This set of simulations uses a Junge model of the aerosol size distribution and a spectrally constant value of the imaginary part of the refractive index which is the parameter that controls the absorption efficiency.

[7] The major originality of NeuroVaria as compared to the SOA is that it uses a variational method to perform this inversion [*Talagrand and Courtier*, 1987] which uses a conjugate gradient algorithm to minimize the difference between the measured and the simulated reflectance spectra. This procedure avoids time-consuming searches and interpolations in the large database of simulated reflectance spectra. A second originality of NeuroVaria is that the simulated reflectance spectrum is computed with an MLP trained with the set of radiative transfer simulations described above. Consequently, the simulation is a differentiable function that allows to perform a conjuguate gradient minimizing algorithm. During the successive iterations, the method adjusts the control parameters of the direct model, such as the aerosol optical thickness τ, which represents the amount of aerosols, the aerosol Ångström exponent α, which is related to the aerosol size, the aerosol single-scattering albedo ω_O, which characterizes the absorption efficiency of aerosols, and the pigment concentration that determines the water leaving reflectance spectrum.

[8] A first validation of the NeuroVaria approach was conducted for non-absorbing aerosols only using in-situ measurements [*Brajard et al.*, 2006b]. The objective of this paper is to present an additional validation of the method in the presence of absorbing aerosols.

2. Data and Methods

[9] The Indian peninsula is an important source of anthropogenic aerosols due to human activity [*Pelon et al.*, 2002]. During the winter Indian Ocean monsoon, the atmospheric circulation transports these aerosols over large distances (600–700km) to the ocean. In February–March 1999, results of the INDian Ocean Experiment (INDOEX) [*Ramanathan et al.*, 2001] showed high absorption levels, with typical values of ω_O between 0.88 and 0.93 [*Léon et al.*, 2002].

[10] NeuroVaria was applied to SeaWiFS images of the Indian Ocean during this period of intense transport of pollutant aerosol from India and results were compared with those obtained with the SeaWiFS standard algorithm. This comparison focuses on τ and $\rho_w(\lambda)$ which is a good indicator of the quality of the atmospheric correction.

[11] NeuroVaria was integrated into the version 4.7 of SeaDAS (http://oceancolor.gsfc.nasa.gov/seadas/). It was applied to SeaWiFS images off India from 1 to 15 March 1999 between 55°E and 95°E and 0°N and 30°N. Figure 1 shows the NeuroVaria retrievals for τ, ω_0, $\rho_w(443)$ and this for $\rho_w(443)$ by the standard algorithm for 2, 7 and 13 March 19.

[12] Maps of the aerosol optical thickness presented in Figure 1 show that the atmospheric situation has evolved rapidly over the 12 days. On 2 March, there was a very dense absorbing aerosol plume between 15°N and 20°N for which the SeaWiFS algorithm failed to compute the atmospheric correction. On 7 March, the aerosol optical thickness was lower in this region (between 0.2 and 0.35) and the two algorithms allow estimating ρ_w. Finally, on 13 March, the plume shifted southward and very few aerosols remained in the atmosphere in the zone of interest, except along the Indian coast.

[13] Maps of ω_0 in Figure 1 show that NeuroVaria detected mostly absorbing aerosols (ω_0 between 0.95 and 0.98), so we could expect the standard algorithm to fail for most pixels. Because the three scenes were taken within a few days, we postulate that oceanic constituents were relatively constant in the open ocean during this period, compared to the atmospheric parameters variability.

3. Improvement in Atmospheric Correction

[14] Maps of $\rho_w(443)$ in Figure 1 are quite similar in areas where there is no absorbing aerosols, i.e., where $\omega_0 \approx 1$, even if standard retrievals are slightly lower. This underestimation dramatically increases in regions where NeuroVaria detects some absorption. In addition, NeuroVaria

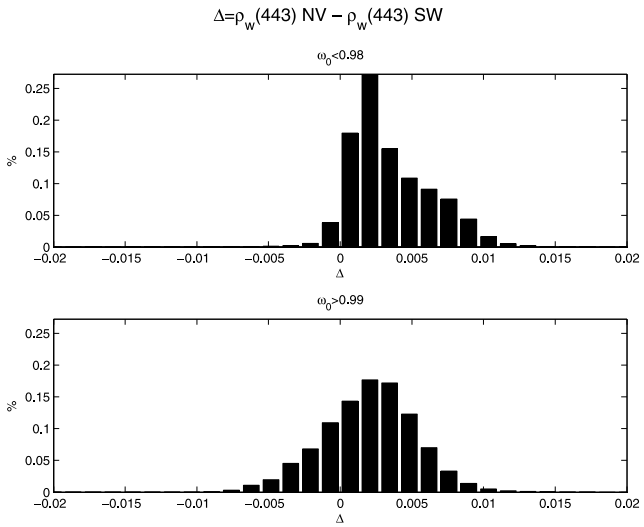

Figure 2. Histograms of the difference Δ between the NeuroVaria retrieval and the standard SeaDas retrieval for $\rho_w(443)$ for the first week of March 1999. The upper histogram has been computed for pixels for which NeuroVaria detected absorbing aerosols ($\omega_0 < 0.98$) and the lower for $\omega_0 > 0.9$. (top) The mean of the first histogram is significatively different from zero (the confidence interval at 5% is [0.0034; 0.0035]) and indicates a systematic underestimation by the standard algorithm. (bottom) The mean of the second histogram is 0.002 which means that the underestimation is smaller where the aerosols are detected to be non-absorbing.

retrievals for the three days are comparable whereas standard retrievals are very different from one day to another which could indicate a failure in the atmospheric correction process for the standard algorithm. These results confirm the assumption that the standard algorithm overestimates the aerosol reflectance in the blue and green in presence of absorbing aerosols. Histograms presented in Figure 2 compare the difference between NeuroVaria and the standard algorithm in case of absorbing aerosols ($\omega_0 < 0.98$) and in case of very low absorbing aerosols ($\omega_0 > 0.99$). These histograms show that the difference between standard and NeuroVaria reflectances are gaussian, with a bias of about 0.0025 for scattering aerosols, whereas it is strongly asymmetric toward low standard values for absorbing aerosols.

[15] Geophysical parameters retrieved by both the NeuroVaria and the SeaWiFS algorithms were extracted along a transect (20°N; 60°E)–(18°N; 73°E), as shown in Figure 1. One hundred pixels were extracted along this transect and for each pixel we computed the mean quantities on a 5 × 5 pixels neighborhood window. In Figure 3, we present the optical thickness and the water-leaving reflectance at 443 and 510 nm, which are respectively the most and the least sensitive bands to phytoplankton concentration, retrieved by both NeuroVaria and SeaWiFS algorithms for the 2, 7 and 13 March 1999.

[16] $\rho_w(443)$ obtained by both methods show a good spatial and temporal stability for the days when there was little or no absorbing aerosols along the transect (7 and 13 March). On the contrary, the two algorithms perform differently on 2 March, NeuroVaria providing stable reflectances, similar to that of 7 and 13 March, whereas the standard algorithm produces very low reflectances as the optical thickness increases. Note that for the three days, the decrease in $\rho_w(443)$ near the coast corresponds to an increase in water absorption due to an increasing phytoplankton concentration. The same conclusion holds for $\rho_w(510)$ (Figure 3), with a decrease of the standard algorithm reflectances on 2 March where the aerosol optical thickness increases.

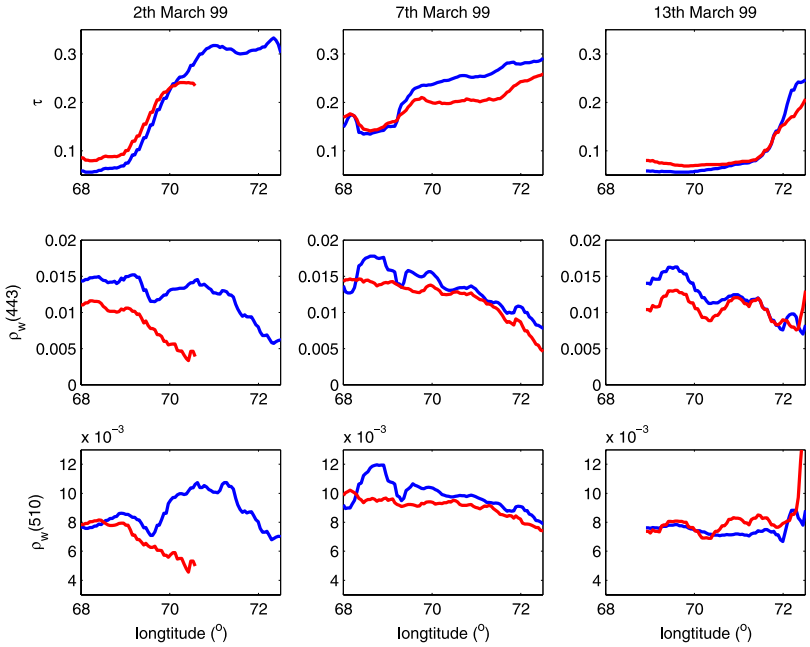

Figure 3. Optical thickness τ, water-leaving reflectance ρ_w at 443 nm and at 510 nm along the transect indicated in Figure 1. The results of the NeuroVaria processing are in blue and those of the standard processing in red.

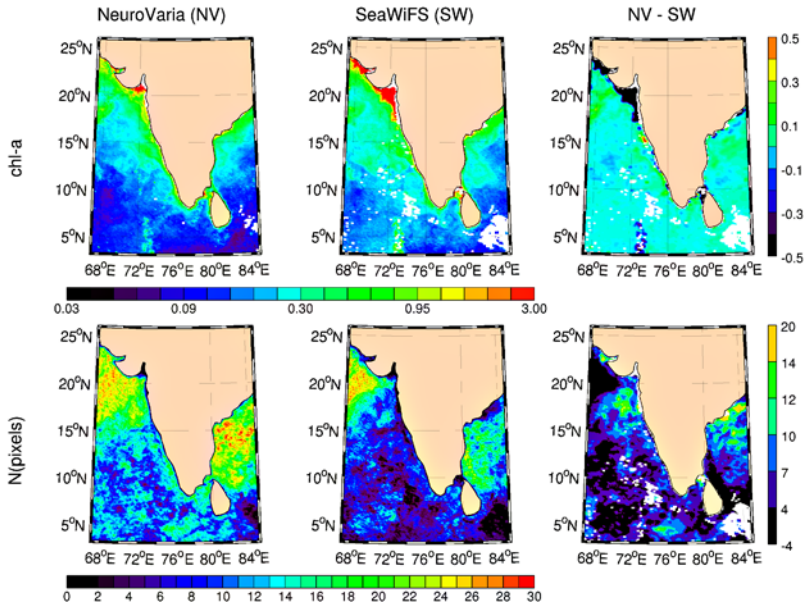

Figure 4. Mean values computed for the two first weeks of March 1999 (left) by NeuroVaria, (middle) by the standard algorithm and (right) the difference between Neurovaria and the standard algorithm. (top) The concentration of chlorophyll-*a* ($mg.m^{-3}$) and (bottom) the number of pixels used to compute the means.

[17] Figure 3 thus shows that for 2 March, the accuracy of the standard algorithm decreases strongly. This algorithm fails to provide estimation of ρ_w in presence of absorbing aerosols where $\tau > 0.25$. This phenomenon is clearly demonstrated for the channels at 443nm and 510nm but also occurs at other wavelengths (not shown). It confirms the conclusions drawn from Figure 1: the strong decrease of ρ_w was not visible for the other days which suggests that it did not correspond to any physical reality. On the contrary, no such decrease was observed in the NeuroVaria retrieval of ρ_w.

4. Impact on Ocean Color Products

[18] Mean chlorophyll-*a* maps were computed on the 9 km × 9 km grid used for SeaWiFS Level-3 GAC products. Retrieved chlorophyll-*a* values were calculated from the ρ_w spectrum with the OC4V4 algorithm [*O'Reilly et al.*, 1998]. Pixels detected as "Bright", "Land" or "Cloud" are excluded. The two algorithms were applied to images of the first two weeks of March 1999 to compute the maps of mean chl-*a* as well as the map of the difference between the two results, as shown in Figure 4.

[19] The two algorithms produce significantly different spatial patterns of chl-*a*, particularly in the oligotrophic region South of 10°N. In this area, NeuroVaria yields lower ($\approx 0.15 mg.m^{-3}$) and more homogeneous values than the standard algorithm ($\approx 0.25\ mg.m^{-3}$), which seems to be highly perturbated by the large plume of absorbing aerosols shown in Figure 1. In addition, the map obtained with NeuroVaria appears less noisy and displays greater details associated with oceanic mesoscale structures. This is partly due to the fact that NeuroVaria yields more stable water-leaving reflectances, but comes also from the fact that this algorithm retrieves a larger number of pixels than the standard algorithm, so that the mean values are statistically more representative and allow a more realistic monitoring of the 2-week period. Except for the North, Figure 4 shows that there is almost a factor of 2 between the number of pixels retrieved by Neurovaria and by the standard algorithm. In the northern part of the images, chl-*a* values obtained with both algorithms appear very comparable. This is likely due to the fact that the aerosol plume stayed for a shorter period of time in this region, so that the number of pixels used to compute these two maps are closer in the North than in the South. Note that chl-*a* values in coastal waters (20°N, 72°E) are systematically higher with the standard algorithm because NeuroVaria in its present form does not allow retrieving chlorophyll-*a* larger than $1 mg.m^{-3}$ [*Brajard et al.*, 2006b].

5. Conclusion

[20] NeuroVaria has been designed to perform accurate atmospheric corrections under very contrasted conditions, including absorbing aerosols, and consequently to improve the retrieval of water constituents in regions where standard algorithms for atmospheric correction fail most of the time. This improved algorithm was applied to SeaWiFS images of the ocean near India during an episode of transport of absorbing aerosols in March 1999. These results were compared with those obtained with the SeaWiFS standard atmospheric correction algorithm. We showed that NeuroVaria removes most of the weaknesses of the standard daily products in the presence of absorbing aerosols and allows to perform accurate atmospheric corrections for optical thicknesses larger than 0.3. These improved performances also allow to process more pixels, which turns out to be very important in such a region where aerosol plumes are frequent and cover large areas. The analysis of maps of mean chlorophyll-*a* over the 2-week period considered here clearly demonstrates the usefulness of NeuroVaria in such specific oceanic regions.

[21] **Acknowledgments.** The authors thank the reviewer for her/his very helpful comments, Michel Crepon for his useful help in the drafting of this paper, H. R. Gordon, for providing the synthetical database, the SeaWiFS project (NASA/GSFC) and Orbimage, for SeaWiFS data and ACRIst, for their support.

References

Banzon, V., R. Evans, H. Gordon, and R. Chomko (2004), SeaWiFS observations of the Arabian Sea southwest monsoon bloom for the year 2000, *Deep Sea Res., Part II*, *51*, 189–208.

Brajard, J., C. Jamet, C. Moulin, and S. Thiria (2006a), Use of a neuro-variational inversion for retrieving oceanic and atmospheric constituents from satellite ocean colour sensor: Application to absorbing aerosols, *Neural Networks*, *19*(2), 178–185.

Brajard, J., C. Jamet, C. Moulin, and S. Thiria (2006b), Validation of a neuro-variational inversion of ocean color images, *Adv. Space Res.*, *38*(2), 2169–2175.

Chomko, R., and H. Gordon (1998), Atmospheric correction of ocean color imagery: Use of the Junge power-law aerosol size distribution with variable refractive index to handle aerosol absorption, *Appl. Opt.*, *37*, 5560–5572.

Chomko, R., and H. Gordon (2001), Atmospheric correction of ocean color imagery: Test of the spectral optimization algorithm with SeaWiFS, *Appl. Opt.*, *40*, 2973–2984.

Gordon, H. (1997), Atmospheric correction of ocean color imagery in the earth observing system era, *J. Geophys. Res.*, *102*, 17,081–17,106.

Gordon, H., and M. Wang (1994), Retrieval of water-leaving radiance and aerosol optical thickness over the oceans with SeaWiFS: A preliminary algorithm, *Appl. Opt.*, *33*, 443–452.

Gordon, H., T. Du, and T. Zhang (1997), Remote sensing of ocean color and aerosol properties: Resolving the issue of aerosol absorption, *Appl. Opt.*, *36*, 8670–8684.

Jamet, C., S. Thiria, C. Moulin, and M. Crepon (2005), Use of a neuro-variational inversion for retrieving oceanic and atmospheric constituents from ocean color imagery: A feasibility study, *J. Atmos. Oceanic Technol.*, *22*(4), 460–475, doi:10.1175/JTECH1688.1.

Léon, J.-F., P. Chazette, J. Pelon, F. Dulac, and H. Randriamiarisoa (2002), Aerosol direct radiative impact over the INDOEX area based on passive and active remote sensing, *J. Geophys. Res.*, *107*(D19), 8006, doi:10.1029/2000JD000116.

Moulin, C., H. R. Gordon, R. M. Chomko, V. F. Banzon, and R. H. Evans (2001), Atmospheric correction of ocean color imagery through thick layers of Saharan dust, *Geophys. Res. Lett.*, *28*, 5–8.

O'Reilly, J. E., S. Maritorena, B. G. Mitchell, D. A. Siegel, K. L. Carder, S. A. Garver, M. Kahru, and C. McClain (1998), Ocean color chlorophyll algorithms for SeaWiFS, *J. Geophys. Res.*, *103*, 24,937–24,953.

Pelon, J., C. Flamant, P. Chazette, J.-F. Leon, D. Tanre, M. Sicard, and S. K. Satheesh (2002), Characterization of aerosol spatial distribution and optical properties over the Indian Ocean from airborne LIDAR and radiometry during INDOEX'99, *J. Geophys. Res.*, *107*(D19), 8029, doi:10.1029/2001JD000402.

Ramanathan, V., et al. (2001), Indian Ocean Experiment: An integrated analysis of the climate forcing and effects of the great Indo-Asian haze, *J. Geophys. Res.*, *106*, 28,371–28,398.

Talagrand, O., and P. Courtier (1987), Variational assimilation of meteorological observations with the adjoint vorticity equation. I: Theory, *Q. J. R. Meteorol. Soc.*, *113*, 1311–1328.

J. Brajard and S. Thiria, LOCEAN, IPSL, Boîte Courier 100, 4, place Jussieu, F-75252 Paris CEDEX 05, France. (julien.brajard@locean-ipsl.upmc.fr)

C. Moulin, LSCE, CEA-Saclay, Bât. 712, F-91191 Gif-sur-Yvette CEDEX, France.